THE JOURNAL OF BIOLOGICAL CHEMISTRY
Vol. 280, No. 14, Issue of April 8, pp. 13987–13992, 2005
Printed in U.S.A.

Comparative Analysis of the Human and Chicken Prion Protein Copper Binding Regions at pH 6.5*[S]

Received for publication, October 18, 2004, and in revised form, January 3, 2005
Published, JBC Papers in Press, January 30, 2005, DOI 10.1074/jbc.M411775200

Lars Redecke‡, Wolfram Meyer-Klaucke§, Mirjam Koker¶, Joachim Clos¶, Dessislava Georgieva‡‖, Nicolay Genov‖, Hartmut Echner, Hubert Kalbacher**, Markus Perbandt‡‡, Reinhard Bredehorst‡‡, Wolfgang Voelter**, and Christian Betzel‡ ‡‡§§**

*From the ‡Center of Experimental Medicine, Institute of Biochemistry and Molecular Biology I, University Hospital Hamburg-Eppendorf, c/o Deutsches Elektronen Synchrotron (DESY), and the §European Molecular Biology Laboratory, Outstation Hamburg at DESY, 22603 Hamburg, Germany, the ¶Bernhard-Nocht-Institute for Tropical Medicine, 20359 Hamburg, Germany, the ‖Institute of Organic Chemistry, Bulgarian Academy of Sciences, Sofia 1113, Bulgaria, the **Institute of Physiological Chemistry, University of Tübingen, 72076 Tübingen, Germany, and the ‡‡Institute of Biochemistry and Food Chemistry, University of Hamburg, 20146 Hamburg, Germany*

Recent experimental evidence supports the hypothesis that prion proteins (PrPs) are involved in the Cu(II) metabolism. Moreover, the copper binding region has been implicated in transmissible spongiform encephalopathies, which are caused by the infectious isoform of prion proteins (PrP^{Sc}). In contrast to mammalian PrP, avian prion proteins have a considerably different N-terminal copper binding region and, most interestingly, are not able to undergo the conversion process into an infectious isoform. Therefore, we applied x-ray absorption spectroscopy to analyze in detail the Cu(II) geometry of selected synthetic human PrP Cu(II) octapeptide complexes in comparison with the corresponding chicken PrP hexapeptide complexes at pH 6.5, which mimics the conditions in the endocytic compartments of neuronal cells. Our results revealed that structure and coordination of the human PrP copper binding sites are highly conserved in the pH 6.5–7.4 range, indicating that the reported pH dependence of copper binding to PrP becomes significant at lower pH values. Furthermore, the different chicken PrP hexarepeat motifs display homologous Cu(II) coordination at sub-stoichiometric copper concentrations. Regarding the fully cation-saturated prion proteins, however, a reduced copper coordination capability is supposed for the chicken prion protein based on the observation that chicken PrP is not able to form an intra-repeat Cu(II) binding site. These results provide new insights into the prion protein structure-function relationship and the conversion process of PrP.

A group of lethal neurodegenerative disorders known as transmissible spongiform encephalopathies are related to prion proteins (PrPs),[1] which are synaptic glycosyl-phosphatidylinositol-anchored surface glycoproteins (1, 2) that are expressed mainly in the central nervous system (3, 4). Prion diseases are apparently caused by conversion of the monomeric 28-kDa cellular prion protein (PrP^{C}) into a pathogenic conformational isoform, usually denoted as the scrapie form, PrP^{Sc} (5, 6). These abnormally folded proteins accumulate into highly protease-resistant aggregates (7) that act as a template for the transition of native PrP^{C} (8). Despite numerous efforts to elucidate the physiological role of the cellular prion protein, its function remains enigmatic. However, the binding of copper to mammalian PrP^{C} *in vivo* and *in vitro* suggests an involvement in copper homeostasis and metabolism (9–11) comprising contributions to endocytotic transport mechanisms (12) as well as neuroprotective pathways (13, 14). Furthermore, the close association of Cu(II) with prion diseases (15–17) emphasizes the need for detailed structural characterization of both PrP isoforms.

The overall structure of recombinant mammalian prion proteins, consisting of a globular C-terminal domain (residues 121 to 231) and a disordered N-terminal tail (residues 23 to 120), are established mainly by NMR investigations (18–21) as well as by two x-ray diffraction studies (22, 23). A total of five high affinity copper binding motifs of PrP^{C} were identified, one at the beginning of the C-terminal domain centered at residues His-96 and His-111 (24, 25) and four within the His-containing sequence PHGGGWGQ that is repeated four times between residues 60 and 91 (9, 10, 26–31). This N-terminal octapeptide repeat region, which is highly conserved in mammals (32, 33), cooperatively binds up to four Cu(II) ions with dissociation constants in the nanomolar to micromolar range, reflecting a significant pH-dependence (9, 26, 31, 34).

Despite the large number of studies, detailed structural models of Cu(II) binding are still discussed. Recently, Morante *et al.* (35) suggested that the coordination shell of Cu(II) varies depending on the occupancy of the available metal sites. This x-ray absorption spectroscopy analysis of bovine octapeptide complexes linked the two common copper binding models, which differ mainly in the number of coordinated imidazole side chains (11,

* This work was supported by Deutsche Luft und Raumfahrtagentur (DLR, Projektträger Gesundheitsforschung) Grant 01KO0206. The costs of publication of this article were defrayed in part by the payment of page charges. This article must therefore be hereby marked "*advertisement*" in accordance with 18 U.S.C. Section 1734 solely to indicate this fact.

[S] The on-line version of this article (available at http://www.jbc.org) contains supplemental material in the form of Tables S-I and S-II presenting EXAFS refinement models of Cu(II) complexes of synthetic peptides derived from human and chicken PrP.

§§ To whom correspondence should be addressed: Inst. of Biochemistry and Food Chemistry, University of Hamburg, Martin-Luther-King Platz 6, 20146 Hamburg, Germany. Tel.: 49-40-8998-4744; Fax: 49-40-8998-4747; E-mail: Betzel@unisgi1.desy.de.

[1] The abbreviations used are: PrP, prion protein; PrP^{C}, cellular isoform of PrP; αHuPrP-(23-231), recombinant PrP corresponding to a human sequence folded into PrP^{C}-like conformation; αChPrP-(24–249), recombinant PrP corresponding to a chicken sequence folded into PrP^{C}-like conformation; MALDI-TOF, matrix-assisted laser desorption ionization time of flight; EXAFS, extended x-ray absorption fine structure; MES, 2-(*N*-morpholino)ethanesulfonic acid.

TABLE I

Cu(II)-complexes of synthetic peptides derived from αChPrP-(24–249) and αHuPrP-(23–231) used for x-ray absorption spectroscopy analysis

Cu(II)-complexes were prepared as described in the experimental section. The Cu(II) saturation was experimentally determined by MALDI-TOF mass spectroscopy.

Peptide	Peptide sequence	Cu(II) sites	Cu(II)/PrP	Cu(II)/repeat
ChPrP-(53–58)	Ac-PHNPGY-NH_2	1	0.5	0.5
ChPrP-(53–64)	Ac-$(PHNPGY)_2$-NH_2	2	1.5	0.75
ChPrP-(53–70)	Ac-$(PHNPGY)_3$-NH_2	3	1.5	0.5
ChPrP-(53–76)	Ac-$(PHNPGY)_4$-NH_2	4	2.0	0.5
HuPrP-(60–67)	Ac-PHGGGWGQ-NH_2	1	0.5	0.5
HuPrP-(60–83)	Ac-$(PHGGGWGQ)_3$-NH_2	3	1.5	0.5
HuPrP-(60–91)	Ac-$(PHGGGWGQ)_4$-NH_2	4	2.0	0.5

26–29, 30, 34). Consequently, a conversion of the inter-repeat binding mode of Cu(II) into an intra-repeat site geometry is proposed once the copper concentration increases (35).

Despite the low sequence identity of ~44% (32), the essential features of mammalian prion proteins are also conserved in chicken PrP (36). Homologous Cu(II) binding capability was identified for the tandem hexapeptide (PHNPGY) repeats located between residues 53 and 94 (31, 34, 37). To date, the particular interest in analyzing and understanding the exact Cu(II) coordination geometry of avian PrP is driven by the fact that prion diseases have, up to now, not been observed for birds (38, 39).

In this study, we present a comparative x-ray absorption spectroscopy analysis of Cu(II) coordination to the corresponding repeat sequences of both chicken and human PrP at pH 6.5. According to the putative involvement of PrP in copper homeostasis, this slightly acidified pH value mimics conditions close to the endocytic compartments of neuronal cells, where Cu(II) might be released (9, 16, 40). The results we obtained revealed that the structure and the coordination of the copper binding sites of human PrP are highly conserved between pH 6.5 and pH 7.4, indicating that the reported pH dependence of Cu(II) binding becomes significant at lower pH values. Although chicken PrP has a considerably different copper binding region, the hexarepeat motifs display a homologue Cu(II) coordination at sub-stoichiometric copper concentrations. In contrast, a reduced copper binding ability is proposed for chicken PrP in the fully cation-saturated state, supporting the hypothesis that human and chicken prion proteins are involved in different physiological functions.

MATERIALS AND METHODS

Peptide Synthesis and Purification—Synthetic peptides representing various fragments of the repeat region of human and chicken prion proteins were synthesized with a Biotronik ECOSN P solid phase automated peptide synthesizer (Eppendorf, Hamburg, Germany) using the Fmoc (9-fluorenyl-methoxycarbonyl) method. After elution from the resin and deprotection, the crude peptides were further purified by reverse phase high performance liquid chromatography and assayed for mass and purity (> 98%) by matrix-assisted laser desorption ionization time of flight (MALDI-TOF) analysis, amino acid analyses, and analytical high performance liquid chromatography. To mimic the peptides within the full-length PrP, all peptides were blocked by *N*-acetyl and amide groups at the N terminus and the C terminus, respectively.

Preparation of Cu(II) Complexes of Synthetic Peptides—For the x-ray absorption spectroscopy measurements, peptide-Cu(II) complexes were prepared by adding an appropriate amount of $CuCl_2$ stock aqueous solution to the synthetic peptides (7.4 nM) in 10 mM MES buffer, pH 6.5. The copper concentration was kept sub-stoichiometric to ensure that all Cu(II) ions were complexed with the ligand. The final solutions were centrifuged, transferred to polyimide foil-covered sample holders of 1-mm thickness, and placed into liquid nitrogen immediately before the measurement. The number of Cu(II) ions that were coordinated to the peptides was analyzed by linear flight MALDI-TOF mass spectrometry using a sinapic acid matrix and a Bruker Autoflex mass spectrometer. Subsequent to the incubation with Cu(II), the corresponding samples were reacted with a 5-fold molar excess of diethyl pyrocarbonate at room temperature for 30 min to flag the histidine residues that were not bound to Cu(II) ions (41). The peptide concentrations were determined using extinction coefficients at 280 nm, which were calculated using 5690 M^{-1} cm^{-1} multiplied by the number of Trp residues and 1280 M^{-1} cm^{-1} multiplied by the number of Tyr residues, respectively (42).

X-ray Absorption Spectroscopy and Data Analysis—X-ray absorption spectroscopy data were recorded at the European Molecular Biology Laboratory beam line X32 (Deutsches Elektronen Synchrotron (DESY), HASYLAB). The DORIS (double Ring Store) storage ring was operated at 4.5 GeV with ring currents in the range of 90–145 mA. A Si(111) double monochromator was used to align the wavelength at the copper K-edge accordingly. The samples were mounted in a two-stage Displex cryostat and kept at ~30 K during the measurement. The x-ray absorption spectra of the Cu(II)-peptide complexes were recorded in the florescence mode using a Canberra 13-element solid state detector over the energy range from 8.765 to 9.655 eV. To obtain comparable statistics, a minimum of 10 scans were collected and averaged for each sample. For data reduction, the EXPROG program package was applied (43). The extracted experimental extended x-ray absorption fine structure (EXAFS) signals were analyzed using the refinement program EXCURV 9.20 (44). This approach allows an *ab initio* calculation of the backscattering functions for the involved ions using the Hedin-Lundqvist complex potentials in the muffin-tin approximation. The initial model is then subjected to a constrained refinement process. All structural parameters that define the geometry of the Cu(II) cluster, including the distances of ligands, the Debye-Waller factors for each shell, the Fermi energy, and the angular parameters associated with the imidazole group, were optimized to fit the experimental data. During the calculations, the internal geometry of the imidazole rings was kept fixed (constrained refinement). Their position relative to the Cu(II) atom is at this stage already well defined by the position of the first shell nitrogen atom and two angular parameters. For further experimental and data analysis details see Binsted *et al.* (44).

RESULTS

We have applied x-ray absorption spectroscopy, in particular EXAFS techniques, to analyze in detail the Cu(II) binding geometry and coordination for mammalian and chicken PrP. Our intention was to obtain three-dimensional information to unravel the functional differences of αChPrP-(24–249) and αHuPrP-(23–231) that are potentially associated with the N-terminal copper binding region. Because of the extremely low solubility of the full-length prion proteins at pH 6.5, in particular in complex with Cu(II), we have analyzed synthetic peptides resembling 1–4 tandem copies of the avian hexarepeat and the human octarepeat, respectively (Table I). To mimic these sequences within the full-length proteins, all peptides were blocked at the N terminus by *N*-acetyl and at the C terminus by amide groups. The copper concentration was kept slightly sub-stoichiometric because of a limitation of x-ray absorption spectroscopy, which requires full saturation of the observable Cu(II) by the ligand to avoid heterogenic spectra caused by free metal ions.

The obtained x-ray absorption near-end structure pattern showed a high similarity for all ChPrP and HuPrP peptide Cu(II) complexes (Fig. 1). The almost identical edge energies of 8990 eV resemble the electronic transitions characteristic of Cu(II) ions (45), indicating an identical Cu(II) oxidation state at pH 6.5. The shapes of the copper K-edges of human and chicken complexes appeared to be almost superimposable. However, a

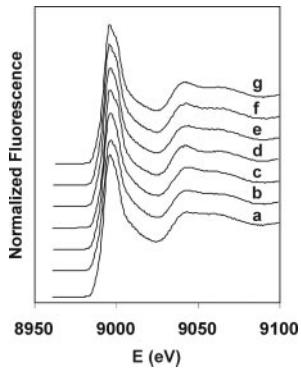

FIG. 1. **Normalized copper K-edge x-ray absorption spectra of Cu(II) bound to selected synthetic peptides of αHuPrP-(23–231) and αChPrP-(24–249).** Displayed *traces* correspond to the following complexes: *a*, Cu(II) HuPrP-(60–67); *b*, Cu(II) HuPrP-(60–83); *c*, Cu(II) HuPrP-(60–91); *d*, Cu(II) ChPrP-(53–58); *e*, Cu(II) ChPrP-(53–64); *f*, Cu(II) ChPrP-(53–70); *g*, Cu(II) ChPrP-(53–76).

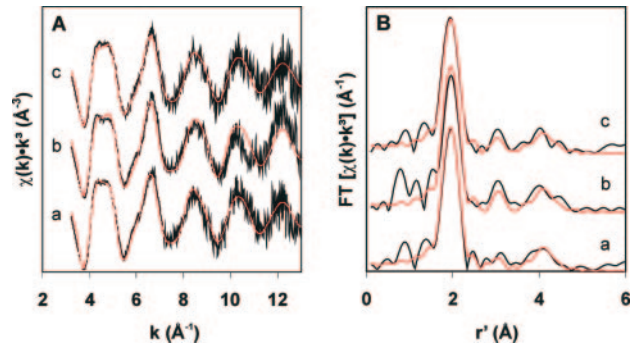

FIG. 2. **EXAFS spectra (*A*) and their Fourier transforms (*B*) of Cu(II) in complex with synthetic peptides derived from αHuPrP-(23–231).** The experimental data (*black lines*) and the model for the backscattering contributions of the nearest atoms obtained by EXCURV 9.20 analysis (*red lines*) are depicted. χ, EXAFS amplitude; *k*, photoelectron wavenumber; *r'*, metal-ligand distance corrected for first shell phase shifts; *FT*, Fourier transform amplitude. For abbreviations of the Cu(II) octarepeat complexes, see the Fig. 1 legend.

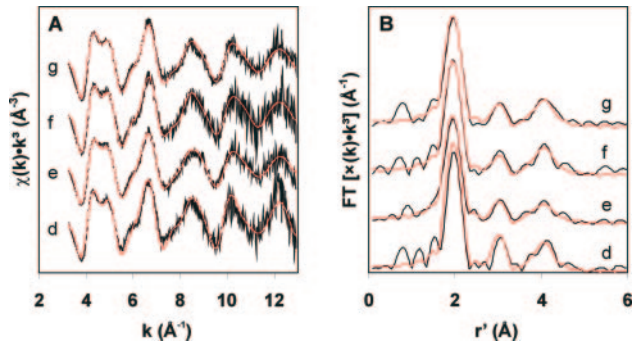

FIG. 3. **EXAFS spectra (*A*) and their Fourier transforms (*B*) of Cu(II) in complex with synthetic peptides derived from αChPrP-(24–249).** The experimental data (*black lines*) and the model for the backscattering contributions of the nearest atoms obtained by EXCURV 9.20 analysis (*red lines*) are shown. χ, EXAFS amplitude; *k*, photoelectron wavenumber; *r'*, metal-ligand distance corrected for first shell phase shifts; *FT*, Fourier transform amplitude. For abbreviations of the Cu(II) hexarepeat complexes see the Fig. 1 legend.

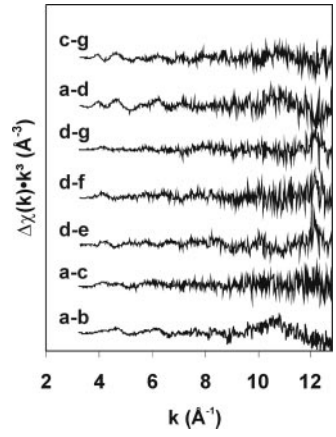

FIG. 4. **Difference spectra of the experimental EXAFS data.** Displayed traces correspond to the Cu(II) complexes of synthetic peptides derived from αHuPrP-(23–231) (*traces a-b* and *a-c*) and αChPrP-(24–249) (*traces d-e*, *d-f*, and *d-g*). Furthermore, the difference spectra of the human and chicken monorepeats (*trace a-d*) and tetrarepeats (*trace c-g*) are displayed. χ, EXAFS amplitude; *k*, photoelectron wavenumber. For abbreviations of the Cu(II) peptide complexes see Fig. 1.

more detailed analysis of the main edge peaks and the first oscillations (9040–9080 eV) revealed distinct differences, which can be assigned to structural changes in the absorber environment of the coordinated Cu(II) ions. The spectra obtained for the chicken complexes are characterized by a split maximum at the edge followed by a slightly humped curve progression (Fig. 1, *traces d–g*). Corresponding spectra of the human Cu(II) peptide complexes containing three and four octarepeats exhibited identical features, although the intensities were reduced significantly (Fig. 1, *traces b–c*). In contrast, the spectrum obtained for the Cu(II)-HuPrP-(60–67) complex showed a single maximum at the copper K-edge and a rather broad, plain oscillation in the 9040–9080 eV region (Fig. 1, *trace a*).

A visual analysis of the extracted experimental k^3-weighted EXAFS spectra and their corresponding Fourier transformations confirmed the existence of three groups of Cu(II) complexes (Figs. 2 and 3). The different shapes of the dominating low frequency signal at 4.5 $Å^{-1}$ in the EXAFS spectra, the different amplitudes of the outer shell peaks at 3.0 and 4.2 Å in the Fourier transforms, and the characteristic unsteady side of the EXAFS peak at 6.5 $Å^{-1}$ (Figs. 2*A* and 3*A*) strongly indicate the presence of histidine ligands in the primary coordination sphere of the copper ions (24, 45, 46).

Cu(II) Site Geometry in the Human Octarepeat Complexes at pH 6.5—As observed for the x-ray absorption near-end structure pattern, the EXAFS spectrum of Cu(II) HuPrP-(60–67) also differs from the spectra obtained for Cu(II) HuPrP-(60–83) and Cu(II) HuPrP-(60–91). This difference is evidenced by small peaks observed in the low frequency region of the corresponding difference spectra, which contain signals caused by the nearest neighbor interactions (Fig. 4, *traces a-b* and *a-c*). However, the spectra of the human Cu(II) peptide complexes containing three and four octarepeat copies are almost superimposable, suggesting a comparable Cu(II) coordination for the octarepeat peptides.

For an initial calculation, the experimental EXAFS spectrum of the Cu(II) HuPrP-(60–67) complex was fitted on the basis of the already known coordination of Cu(II) in complex with mammalian PrP octarepeats at pH 7.4 (11, 35). As a result, the initial models were composed of one to four imidazole groups as well as an appropriate moiety of oxygen/nitrogen ligands to match the typical coordination numbers of Cu(II) ranging from four to six. Based on maximum agreement, constrained refinement indicated that the first coordination shell of Cu(II) in complex with HuPrP-(60–67) at pH 6.5 is formed by one nitrogen atom assigned to an imidazole group and three other light single-bonded nitrogen or oxygen atoms (Fig. 2 and Table II). The consistent distance values of 1.97 ± 0.01 Å are as expected for a Cu(II)-nitrogen coordination (47). Further refinement of the oxygen/nitrogen magnitude is prevented by the high similarity of the nitrogen and oxygen backscattering amplitude as

TABLE II

EXAFS refinement parameters of the best fitting structural models for Cu(II) ions in complex with synthetic peptides derived from αChPrP-(24–249) and αHuPrP-(23–231)

EXAFS spectra were analyzed using the EXCURV 9.20 program package (43). *N*, number of atoms; *r*, distance; $2\sigma^2_{DW}$, Debye-Waller parameter; ΔE_F, shift of the Fermi energy with E_0 = 8979 eV; *R*, *R*-factor; N_{HIS}, number of His residues coordinated to Cu(II). Values in parenthesis represent the 2σ error level. For EXAFS refinement parameters of structural models assuming additional remote oxygen ligands, see the supplemental data in the on-line version of this article.

Cu(II) complexes	Ligands	*N*	*r*	$2\sigma^2_{DW}$	ΔE_F	R^a	N_{HIS}
			Å	*Å²*	*eV*	*%*	
ChPrP-(53–58)	Cu-N/O	4	1.98(1)	0.005(2)[b]	−8(1)	34.4	2.0(3)
ChPrP-(53–64)	Cu-N/O	4	1.97(1)	0.008(2)[b]	−8(1)	21.0	2.0(2)
ChPrP-(53–70)	Cu-N/O	4	1.97(1)	0.007(1)[b]	−8(1)	30.9	2.3(4)
ChPrP-(53–76)	Cu-N/O	4	1.98(1)	0.007(3)[b]	−8(2)	24.4	2.1(2)
HuPrP-(60–67)	Cu-N/O	4	1.97(1)	0.008(2)[b]	−9(1)	28.1	1.3(3)
HuPrP-(60–83)	Cu-N/O	4	1.98(1)	0.006(1)[b]	−9(2)	32.1	2.1(2)
HuPrP-(60–91)	Cu-N/O	4	1.96(2)	0.009(3)[b]	−8(1)	28.9	1.8(2)

[a] The *R*-factor reflects the goodness of the fit.
[b] Constrained to have the same value during refinement for similar atom types.

well as phase functions. The optimal *R*-factor of 0.28 increased significantly if the coordination number was modified further, suggesting a four-atom copper coordination for the single octarepeat peptide.

Utilizing the parameters calculated for the monorepeat, a comparable but slightly different tetragonal Cu(II) coordination was proposed by fitting the EXAFS signals of the Cu(II) HuPrP-(60–83) and Cu(II) HuPrP-(60–91) complexes independently. The data obtained from these complexes, which contain a higher number of octarepeat copies, support the coordination of two imidazole groups to a single Cu(II) ion. Thereby, the amount of oxygen/nitrogen ligands is reduced without affecting the coordination number (Fig. 2). The refined distance values are summarized in Table II and are in the expected range. The marginal variation of the corresponding *R*-factors is caused by minor differences in the signal-to-noise ratios of the detected spectra.

In addition, the assumption of an additional Cu(II) coordination by a remote oxygen ligand (*e.g.* from a water molecule) did not result in a significant decrease of the associated *R*-factors for all human octarepeat Cu(II) complexes (see supplemental data in the on-line version of this article). The exceptionally high Debye-Waller factors obtained for these scenarios indicate that such coordination is unlikely. However, it cannot be fully rejected.

Cu(II) Site Geometry in the Chicken Hexarepeat Complexes at pH 6.5—In contrast to the human Cu(II)-complexes, the detailed analysis of the EXAFS difference spectra of Cu(II) ChPrP-(53–58), Cu(II) ChPrP-(53–64), Cu(II) ChPrP-(53–70), and Cu(II) ChPrP-(53–76) suggested an almost identical Cu(II) coordination sphere among the chicken repeat complexes at pH 6.5 (Fig. 4, *traces d-e*, *d-f*, and *d-g*). On the other hand, comparison with spectra of the human mono-octarepeat and tetra-octarepeat Cu(II) complexes showed significant differences in the low frequency region, where the imidazole groups mainly contribute (Fig. 4, *traces a-d*, *c-g*). The increased amplitude of the outer shell peaks observed in the corresponding Fourier transform spectra are, most probably, connected with changes in the magnitude and orientation of coordinated histidine side chains (46).

The EXAFS data of the Cu(II) ChPrP-(53–58) complex were initially fitted using the geometric parameters previously determined for the human mono-octarepeat as a starting model. The best results were again obtained considering a tetragonal assembly of ligands at a distance of 1.98 ± 0.01 Å. For this configuration, the *R*-factor improved significantly after replacing one light oxygen/nitrogen atom from the first shell by contributions of an additional imidazole group. Therefore, the postulated coordination sphere contains two imidazole groups and two light oxygen/nitrogen atoms (Fig. 3 and Table II). Considering the experimental standard deviations, this model is appropriate for all Cu(II) chicken hexarepeat complexes. Consequently, almost identical Cu(II) binding geometry and coordination were expected for all chicken hexarepeats. Again, the coordination of an additional remote axial oxygen ligand appears to be rather unlikely, although it cannot be fully excluded for chicken complexes at pH 6.5 as well (see supplemental data in the on-line version of this article).

DISCUSSION

Our results suggest that the structure of Cu(II) binding to the selected human octarepeat peptides differs only in the amount of involved histidine residues, depending on the number of repeat copies present within a single peptide. This is indicated by the EXAFS data and by the qualitative analysis of the corresponding x-ray absorption near-end structure pattern. Moreover, the essential mode of copper binding to the octarepeats of human PrP^C at pH 6.5 was found to be highly conserved regarding the already established models proposed for a pH of 7.4 (27, 34, 35). This suggestion is initially supported by the fundamental agreement of the simulated solution structure of the Cu(II)-HuPrP-(60–67) complex (Fig. 5*A*) containing the mono-octarepeat sequence with the crystallographic model of the Cu(II)-HGGGW complex determined at physiological pH conditions (11). Both structures consistently indicate an intra-repeat Cu(II) motif that involves the equatorial coordination of a single His residue as well as three nitrogen/oxygen ligands provided by the peptide backbone. Taking into account the sterical constraints caused by the planarity of the peptide chain, the nitrogen/oxygen-atoms observed by EXAFS most likely correspond to the ligands determined in the crystallographic structure (11). Consequently, the coordination pattern of the Cu(II) ion was apparently not affected by the slightly acidified conditions, indicating that the reported pH dependence of copper binding to PrP (28, 30) becomes significant at pH values below 6.5.

On the other hand, a conversion of the intra-repeat to an inter-repeat Cu(II) site was supposed within the Cu(II) complexes of human peptides containing three and four octarepeats. Considering the sub-stoichiometric copper concentration, this observation is again consistent with a model of cooperative Cu(II)-binding proposed at pH 7.4 (35). The comparable inter-repeat site geometry is featured by the direct engagement of two His residues in equatorial positions, whereas a tetragonal coordination sphere is most likely retained (Fig. 5*B*). According to previous investigations, which support the similarity of Cu(II) binding to peptides containing four octarepeats as well as to PrP^C, the observed inter-repeat

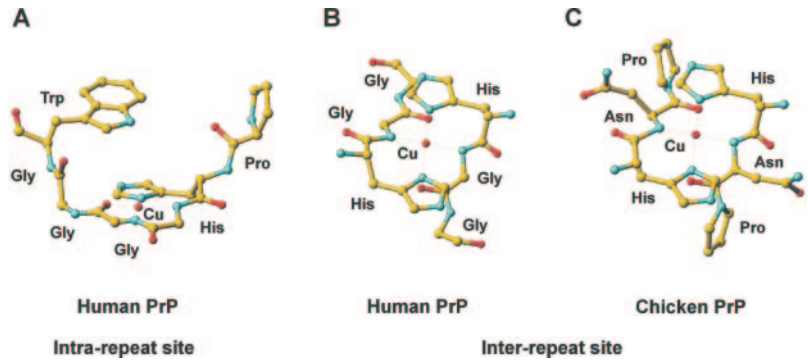

FIG. 5. **Structural model of the Cu(II) coordination to the octarepeat and hexarepeat sequences of human and chicken PrP.** The intra-repeat Cu(II) site geometry (*A*) is proposed for Cu(II) ions bound to HuPrP-(60–67) at pH 6.5. In contrast, for human peptides containing more than two repeat copies, an inter-repeat Cu(II) coordination (*B*) is most likely at sub-stoichiometric copper concentrations, which appears to be homologous to the Cu(II) binding geometry consistently supposed for the chicken Cu(II) hexarepeat complexes (*C*). For all three models, binding of an additional remote oxygen ligand cannot be excluded.

coordination geometry is presumably also applicable to the full-length prion protein (30, 33, 35).

Furthermore, we have to point out that the majority of studies report a penta-coordination of Cu(II) in the intra- as well as in the inter-repeat geometry, considering the presence of an additional axially bound solvent water molecule at a distance of ~2.4 Å (11, 35). Because of the relatively low contributions of an outer shell ligand to the EXAFS signal, we cannot exclude a penta-coordination geometry of the Cu(II) ions via solvent. In fact, the presence of an additional remote water ligand does not alter the proposed structural models significantly. However, based on the present refinement data, the coordination of further remote oxygen ligands appears to be rather unlikely.

Despite the observation that Cu(II) also binds specifically to the hexapeptide repeats (PHNPGY) located in the N-terminal region of the chicken PrP (14), so far only minor attention has been paid to analyzing these hexapeptide Cu(II) binding motifs of avians. Therefore, no detailed structural models characterizing the exact Cu(II) coordination have been proposed to date. Most striking is the altered sequence of these hexarepeats compared with human octarepeats. Because of the remarkably high proportion of proline residues, a structure that is not characteristic for random coil is proposed for the copper-free form of the avian PrP repeats (31, 34). Based on sterical constraints, Pro residues are also known to act as "break-points" in the coordination of donor centers of the peptide chain to metal ions (49). In particular, the presence of Pro at position 4 in the chicken hexapeptide excludes the involvement of a second amide nitrogen in the Cu(II) coordination, as is observed for mammalian mono-octarepeats (11, 27, 34, 35). As a result, the coordination of Cu(II) to the chicken hexapeptides is supposed to follow a different specific pattern (34, 36).

Initially, these restraints are in agreement with our reported results. A Cu(II) binding geometry close to the intra-repeat motif of the human mono-octarepeat was not supported by our investigations. On the contrary, all Cu(II) complexes of the chicken hexarepeats consistently showed an almost identical tetragonal Cu(II) coordination apparently involving two histidine residues to bind one copper ion. Based on the similar x-ray absorption near-end structure spectra, we suggest that this Cu(II) coordination is almost comparable with the inter-repeat binding site of the human peptides, considering the modification that the required amide nitrogen atoms are most probably provided by the adjacent asparagine residues. The coordination of other ligands, including the phenolate oxygen atom of tyrosine, is unfavorable because of sterical constraints. The proposed model for Cu(II) binding (Fig. 5*C*), which can be both intramolecular and intermolecular in the full-length chicken PrP, is also supported by circular dichroism experiments (34).

In conclusion, considering the pH of 6.5 as well as the sub-stoichiometric copper concentrations, we propose almost identical coordination spheres for Cu(II) ions bound to human and chicken prion peptides containing more than two repeat copies, which is consistent with the model of Cu(II) sites proposed for human PrP^C at a pH of 7.4 (35). This remarkable result is most likely depending on the available copper concentration. With regard to human PrP, a cooperative Cu(II) binding process is observed at pH 7.4 (11, 28, 34), which is reflected by the formation of a high number of intra-repeat sites once the copper content is increased up to full site occupancy (35). This characteristic feature is potentially preserved together with the overall ligand geometry in human PrP at pH 6.5. However, intra-repeat Cu(II) binding modes are assumed to be prevented in chicken PrP because of the additional proline residue within the hexarepeat sequence. Consequently, the copper coordination is supposed to differ significantly between the fully cation-loaded human and chicken PrPs. This assumption is in agreement with investigations performed at high copper concentrations, which reported a significantly reduced number of copper ions bound to chicken PrP compared with human PrP (31, 34).

The analysis of the prion copper binding sites provides a structural basis for a putative pH-dependent molecular switch that governs the uptake and release of Cu(II) within the proposed copper metabolism (9–11). Our results evolved at a pH of 6.5, which is close to conditions in the endocytic compartments of neuronal cells where the Cu(II) is potentially released, closing the gap between the detailed structural models determined at pH 7.4 and the studies performed at pH 6.0 (48). In addition, the reduced ability of copper binding suggested for the chicken PrP at high Cu(II) concentrations in the environments of membrane rafts is highly indicative of different physiological functions of human and chicken prion proteins. Furthermore, the absence of prion diseases in chicken, which are shown to be closely associated with changes of the copper content within the neuronal cells (15–17), appears to be related to the differences in the Cu(II) coordination between human and avian prion proteins.

REFERENCES

1. Stahl, N., Borchelt, D. R., Hsiao, F., and Prusiner, S. B. (1987) *Cell* **51,** 229–240
2. Caughey, B. W., Dong, A., Bhat, K. S., Ernst, D., Hayes S. F., and Caughey, W. S. (1991) *Biochemistry* **30,** 7672–7680
3. Sales, N., Rodolfo, K., Hassig, R., Faucheux, B., Di Giamberardino, L., and Moya, K. L. (1998) *Eur. J. Neurosci.* **10,** 2464–2471
4. Kretzschmar, H. A., Prusiner, S. B., Stowring, L. E., and DeArmond, S. J. (1986) *Am. J. Pathol.* **122,** 1–5
5. Bolton, D. C., McKinley, M. P., and Prusiner, S. B. (1982) *Science* **218,** 1309–1311
6. Prusiner, S. B., Bolton, D. C., Groth, D. F., Bowman, K. A., Cochran, S. P., and McKinley, M. P. (1982) *Biochemistry* **21,** 6942–6950
7. McKinley, M. P., Bolton, D. C, and Prusiner, S. B. (1983) *Cell* **35,** 57–62
8. Büeler, H., Fischer, M., Lang, Y., Bluethmann, H., Lipp, H.-P., DeArmond, S. J., Prusiner, S. B., Auet, M., and Weissmann, C. (1992) *Nature* **356,** 577–582
9. Kramer, M. L., Kratzin, H. D., Schmidt, B., Römer, A., Windl, O., Liemann, S., Hornemann, S., and Kretzschmar, H. (2001) *J. Biol. Chem.* **276,** 16711–16719
10. Aronoff-Spencer, E., Burns, C. S., Avdievich, N. I., Gerfen, G. J., Peisach, J., Antholine, W. E., Ball, H. L., Cohen, F. E., Prusiner, S. B., and Millhauser, G. L. (2000) *Biochemistry* **39,** 13760–13771

11. Burns, C. S., Aronoff-Spencer, E., Dunham, C. M., Lario, P., Avdievich, N. I., Antholine, W. E., Olmstead, M. M., Vrielink, A., Gerfen, G. J., Peisach, J., Scott, W. G., and Millhauser, G. L. (2002) *Biochemistry* **41,** 3991–4001
12. Pauly, P. C., and Harris, D. A. (1998) *J. Biol. Chem.* **273,** 33107–33110
13. Rachidi, W., Vilette, D., Guiraud, P., Arlotto, M., Riondel, J., Laude, H., Lehmann, S., and Favier, A. (2003) *J. Biol. Chem.* **278,** 9064–9072
14. Brown, D. R., Wong, B. S., Hafiz, F., Clive, C., Haswell, S. J., and Jones, I. M. (1999) *Biochem. J.* **344,** 1–5
15. Brown, D. R. (2001) *Brain Res. Bull.* **55,** 165–173
16. Lehmann, S. (2002) *Curr. Opin. Chem. Biol.* **6,** 187–192
17. Millhauser, G. L. (2004) *Acc. Chem. Res.* **37,** 79–85
18. Zahn, R., Liu, A., Luhrs, T., Rieck, R., von Schroetter, C., Lopez Garcia, F., Billeter, M., Calzolai, L., Wider, G., and Wüthrich, K. (2000) *Proc. Natl. Acad. Sci. U. S. A.* **97,** 145–150
19. Riek, R., Hornemann, S., Wider, G., Billeter, M., Glockshuber, R., and Wüthrich, K. (1996) *Nature* **382,** 180–182
20. James, T. L., Liu, H., Ulyanov, N. B., Farr-Jones, S., Zhang, H., Donne, D. G., Kaneko, K., Groth, D., Mehlhorn, I., Prusiner, S. B., and Cohen, F. E. (1997) *Proc. Natl. Acad. Sci. U. S. A.* **94,** 10086–10091
21. Lopez-Garcia, F., Zahn, R., Riek, R., and Wüthrich, K. (2000) *Proc. Natl. Acad. Sci. U. S. A.* **97,** 8334–8339
22. Knaus, K. J, Morillas, M., Swietnicki, W., Malone, M., Surewicz, W. K., and Yee, V. C. (2001) *Nat. Struct. Biol.* **8,** 770–774
23. Haire, L. F., Whyte, S. M., Vasisht, N., Gill, A. C., Verma, C., Dodson, E. J., Dodson, G. G., and Bayley, P. M. (2004) *J. Mol. Biol.* **336,** 1175–1183
24. Hasnain, S. S., Murphy, L. M., Strange, R. W., Grossmann, J. G., Clarke, A. R., Jackson, G. S., and Collinge, J. C. (2001) *J. Mol. Biol.* **311,** 467–473
25. Jones, C. E., Abdelraheim, S. R., Brown, D. R., and Viles, J. H. (2004) *J. Biol. Chem.* **279,** 32018–32027
26. Jackson, G. S., Murray, I., Hosszu, L. L. P., Gibbs, N., Waltho, J. P., Clarke, A. R., and Collinge, J. (2001) *Proc. Natl. Acad. Sci. U. S. A.* **98,** 8531–8535
27. Burns, C. S., Aronoff-Spencer, E., Legname, G., Prusiner, S. B., Antholine, W. E., Gerfen, G. J., Peisach, J., and Millhauser, G. L. (2003) *Biochemistry* **42,** 6794–6803
28. Viles, J. H., Cohen, F. E., Prusiner, S. B., Goodin, D. B., Wright, P. E., and Dyson, H. J. (1999) *Proc. Natl. Acad. Sci. U. S. A.* **96,** 2042–2047
29. Quin, K., Yang, D. S., Yang, Y., Chishti, M. A., Meng, L.-J., Kretzschmar, H. A., Yip, C. M., Fraser, P. E., and Westaway, D. (2000) *J. Biol. Chem.* **275,** 19121–19131
30. Stockel, J., Safar, J., Wallace, A. C., Cohen, F. E., and Prusiner, S. B. (1998) *Biochemistry* **37,** 7185–7193
31. Hornshaw, M. P., McDermott, J. R., Candy, J. M., and Lakey J. H. (1995) *Biochem. Biophys. Res. Commun.* **214,** 993–999
32. Schätzl, H. M., Da Costa, M., Taylor, L., Cohen, F. E., and Prusiner, S. B. (1995) *J. Mol. Biol.* **245,** 362–374
33. Wopfner, F., Weidenhofer, G., Schneider, R., von Brunn, A., Gilch, S., and Schwarz, T. F. (1999) *J. Mol. Biol.* **289,** 1163–1178
34. Garnett, A. P., and Viles, J. H. (2003) *J. Biol. Chem.* **278,** 6795–6802
35. Morante, S., Gonzalez-Iglesias, R., Potrich, C., Meneghini, C., Meyer-Klaucke, W., Minestrina, G., and Gasset, M. (2004) *J. Biol. Chem.* **279,** 11753–11759
36. Marcotte, E. M., and Eisenberg, D. (1999) *Biochemistry* **38,** 667–676
37. Hornshaw, M. P., McDermott, J. R., and Candy, J. M. (1995) *Biochem. Biophys. Res. Commun.* **207,** 621–629
38. Matthews, D., and Cooke, B. C. (2003) *Rev. Sci. Tech.* **22,** 283–296
39. Narang, H. (1997) *Vet. Rec.* **141,** 255–256
40. Miura, T., Hori-i, A., Mototani, H., and Takeuchi, H. (1999) *Biochemistry* **38,** 11560–11569
41. Qin, K., Yang, Y., Mastrangelo, P., and Westaway, D. (2002) *J. Biol. Chem.* **277,** 1981–1990
42. Gill, S. C., and von Hippel, P. H. (1989) *Anal. Biochem.* **182,** 319–326
43. Nolting, H. F., and Hermes, C. (1993) *EXPROG: EMBL EXAFS Data Analysis and Evaluation Program for PC/AT*, European Molecular Biology Laboratory, Hamburg, Germany
44. Binsted, N., Strange, R. W., and Hasnain, S. S. (1992) *Biochemistry* **31,** 12117–12125
45. Arnesano, F., Banci, L., Bestini, I., Mangani, S., and Thompsett, A. R. (2003) *Proc. Natl. Acad. Sci. U. S. A.* **100,** 3814–3819
46. Steiner, R. A., Meyer-Klaucke, W., and Dijkstra, B. W. (2002) *Biochemistry* **41,** 7963–7968
47. Harding, M. M. (2001) *Acta Crystallogr. Sect. D Biol. Crystallogr.* **57,** 401–411
48. van Doorslaer, S., Cereghetti, G. M., Glockshuber, R., and Schweiger, A. (2001) *J. Phys. Chem.* **105,** 1631–1639
49. Bataille, M., Formicka-Kozlowska, G., Kozlowski, H., Pettit, L. D., and Steel, I. (1984) *J. Chem. Soc. Chem. Commun.* 231–232